

Cite this: *Lab Chip*, 2012, **12**, 317

www.rsc.org/loc

PAPER

An integrated chip for immunofluorescence and its application to analyze lysosomal storage disorders

Jie Shen,^a Ying Zhou,^a Tu Lu,^b Junya Peng,^b Zhixiang Lin,^b Lei Huang,^{bc} Yuhong Pang,^a Li Yu^b and Yanyi Huang^{*ad}

Received 4th September 2011, Accepted 21st October 2011

DOI: 10.1039/c1lc20845d

Immunofluorescence (IF) is a common method to observe protein distribution and localization at the single-cell level through wide-field fluorescence or confocal microscopy. Conventional protocol for IF staining of cells typically requires a large amount of reagents, especially antibodies, and noticeable investment in both labor and time. Microfluidic technologies provide a cost-effective alternative: it can evaluate and optimize experimental conditions, and perform automatic and high-throughput IF staining on-chip. We employed this method to analyze lysosomal storage disorders (LSDs) based on the expression and morphological distribution of LAMP1 and LC3 in starving cells. With pneumatic valves integrated on-chip, the parallel staining process can be completed within a few hours. The total consumption of each antibody solution for the whole experiment is merely 0.3 μ L. This device provides a promising tool for automated high-throughput molecular imaging at cell level that can be applied for diagnostic analysis.

Introduction

Immunofluorescence (IF), with high sensitivity and specificity, has been used for various applications including the observation of subcellular distribution of biomolecules and specific metabolites.^{1,2} It has been regarded as a routine technique in basic biomedical research and more recently, applied to clinical diagnosis.³ Typically, the specific proteins or molecules in cell organelles are stained with fluorescent-labeled antibodies and the fluorescent images are observed with wide-field fluorescence or confocal microscopes.⁴ The morphology and the sizes of organelles are usually subject to certain pathological conditions, making themselves great markers for various diseases, such as autophagy-related life processes.⁵ Autophagy, a major lysosome cargo delivery pathway, has been shown to be highly related to lysosomal storage disorders (LSDs),⁶ a group of genetic diseases mostly resulted from the deficiency of one or more specific lysosomal hydrolases.^{7–9} The image-based LSDs analysis may help differentiating the complex subgroups of the diseases and providing accurate diagnosis swiftly.

The standard IF assay uses highly specific primary antibodies to bind the antigens of interest in cells, and then uses secondary antibodies, conjugated with fluorescent dyes, to recognize the bound primary antibodies.¹⁰ However, the conventional method consumes a considerable amount of samples, with a tedious process for sample treatment and result analysis. Microfluidic technology has shown promising potential as a cost-effective platform for biological analysis by lowering the consumption of samples and reagents, and by reducing experimental errors through automatic operation.^{11–13} Using a highly integrated microfluidic device, multi-step experiments, with highly accurate liquid manipulation, can be carried out in parallel.^{14–17} Although detailed sub-cellular imaging analysis through IF are still mostly done by conventional methods, recently it has been realized in the microfluidic channels for carrying out immunoassays,^{18–22} monitoring gene expression,^{23,24} observing cell phenotypes,^{25,26} as well as performing high-throughput²⁷ and high-content screenings²⁸ on-chip.

In this paper, we report an integrative microfluidic approach to rapidly perform highly parallel IF experiments, including multiple programmable reactions and washing steps. We performed a high-throughput IF assay with different cell lines cultured on-chip, and screened for optimal experimental conditions. The device was fabricated to be compatible with confocal microscopy, providing high-quality cell IF images. Only a small amount of cells, typically a few hundreds, are needed for each experiment. We have applied this device to human fibroblast and LSDs cell lines with lysosomal-associated membrane protein 1 (LAMP1)^{29,30} and microtubule-associated protein 1 light chain

^aCollege of Engineering, and Biodynamic Optical Imaging Center (BIOPI), Peking University, Beijing, 100871, China. E-mail: yanyi@pku.edu.cn

^bSchool of Life Sciences, Tsinghua University, Beijing, 100084, China

^cCenter of Biomedical Analysis, Tsinghua University, Beijing, 100084, China

^dCollege of Chemistry and Molecular Engineering, Peking University, Beijing, 100871, China

3 (LC3)³¹ staining. With at least 100-fold reduction of the consumption of antibodies, the results obtained from chips have the same quality as those generated by conventional staining process on glass slides. Moreover, the chip-based approach also ensures identical conditions for comparison between groups. Imaging processing and analysis of these information-rich images can also help us to better differentiate one particular disease from others by clustering through a few key parameters.

Materials and methods

Fabrication of the microfluidic IF chips

Microfluidic IF chips were manufactured using polydimethylsiloxane (PDMS, RTV 615 kit, GE Advanced Materials, USA) as described previously.³² Two separated master molds, one for the fluidic layer and the other for the control layer, were fabricated by photolithography. The silicon wafers were treated with hexamethyldisilazane (Alfa Aesar, USA) vapor for 3 min at 25 °C before being coated with photoresist. The mold of the control layer had 15 μm thick features made by AZ P4620 positive photoresist (AZ Electronic Materials, USA). The mold of fluidic layer was fabricated by spin-coating positive photoresist twice to a final thickness of 24 μm, and the patterned photoresist was re-flowed to obtain a rounded cross section. Before the fabrication of PDMS chips, both molds were treated with trimethylchlorosilane (Sinopharm, China) vapor for 5 min at 25 °C. The control layer was made by pouring PDMS (5 : 1, elastomer to crosslinker ratio) onto its mold to a thickness of 5 to 7 mm. The fluidic layer of the chip was made by spin-coating PDMS (20 : 1, elastomer to crosslinker ratio) onto the mold at 1200 rpm for 60 s. Then the control and fluid layers were baked at 80 °C for 20 min and 30 min, respectively. After the control layer was peeled off from its mold and hole-punched, it was aligned over the fluidic layer, and then bonded at 80 °C for 45 min. The bonded layers were peeled off from the fluid mold, hole-punched, then placed on a cover glass (thickness 0.17 mm) with a thin, cured PDMS layer (10 : 1, elastomer to crosslinker ratio). Finally, the whole chip was incubated at 80 °C for at least 6 h.

Automation

All integrated pneumatic valves in the chips were driven by a series of computer-controlled solenoid valves through home-developed Labview programs. The air pressure for actuating integrated valves was 0.1 MPa, and the pressure for driving liquid sample was 0.01–0.02 MPa.

Cell culture

We used normal rat kidney (NRK) cells, stable clones of YFP-LC3-transfected epithelial cells, 15 lysosomal storage disorders cell lines (GM00156, GM00798, GM01256, GM02438, GM00852, GM00863, GM03030, GM00151, GM00244, GM00636, GM00654, GM00059, GM00110, GM11473 and GM00039 from the Coriell Institute, Camden, NJ, USA), and wild type NIH-3T3 fibroblast cells for experiments. All cells were cultured in Dulbecco's modified Eagle's medium (DMEM, Invitrogen, USA) supplemented with 10% (v/v) fetal bovine

serum (FBS, Invitrogen) and 1% penicillin-streptomycin (Invitrogen) in a humid incubator containing 5% CO₂ at 37 °C.

Cell culture on chips

Before loading cells, the chambers/channels on chip were incubated with 100 μg mL⁻¹ sterilized fibronectin (Invitrogen) for at least 1 h and then rinsed with the culture medium. The cells were trypsinized to single cells, centrifuged, re-suspended, and then seeded into the chambers. The fresh medium was automatically changed into the fluid channels every 4 h, and the cells were maintained in the chamber for 8 to 10 h until fully attached and spread. The whole chip was kept in a homemade culture box which supplied a humid atmosphere containing 5% CO₂ at 37 °C. Before being stained with LC3 and LAMP1, the cells were serum starved for 4 h. To acquire time-lapse images of LC3 expression dynamics, we sequentially fixed the cells at 1 h interval by introducing the fixation solution into each individual chamber.

Microfluidic IF staining

We screened the staining conditions on-chip including various concentrations of primary and secondary antibodies, as well as different concentrations of detergents, such as saponin (Sigma, USA) and Tween 20 (Sinopharm, China), in the solution when permeabilizing and washing cells. Once the optimized staining conditions were fixed, the fixing, blocking, washing and staining processes were carried out automatically on-chip through a Labview program. The chambers were flushed with phosphate buffered saline (PBS, pH 7.4) for 1 min, and then the 4% w/w paraformaldehyde solution in PBS was added to fix cells for 10 min at 25 °C. After fixation, the cells were rinsed with PBS, and blocked with 0.1% saponin and 10% FBS in PBS for 15 min. Then the cells were incubated with the primary antibody of either LAMP1 (Sigma) or GFP (Roche, Germany), or the mixed primary antibodies of LAMP1 and LC3 (Medical & Biological Laboratories, Japan) for 30 min. For each IF staining experiment, a parallel set of cells was stained with blank media as the control. The cells were rinsed with 1% Tween 20, 0.1% saponin, and 10% FBS in PBS and then stained with the secondary antibody. For single staining of LAMP1, the secondary antibody we used was either FITC conjugated IgG (Dingguo Biotechnology, China) or TRITC conjugated IgG (Dingguo Biotechnology). For single staining of GFP to obtain the time-lapse images of LC3, the secondary antibody we used was TRITC conjugated IgG. For LAMP1 and LC3 double staining, the mixed solution of FITC and TRITC conjugated IgG was used. After incubation with the secondary antibody for 45 min, the chambers were rinsed with 10% FBS in PBS. The chip can be directly imaged under a confocal microscope (LSM 710, Zeiss, Germany).

Results and discussion

Chip design and experimental condition optimization

Successful IF staining relies on proper fixation and washing, as well as the right concentrations of the primary and secondary antibodies to retain cellular distribution of the antigen and to preserve cell morphology. However, conventional protocols usually require large volumes of samples and reagents. Most

protocols are also time and labor consuming, which makes them unsuitable for screening a large number of experimental conditions. Various studies have demonstrated that microfluidics is a promising platform for cost-effective, rapid and sensitive bioanalysis.^{11,15}

We fabricated two different integrated microfluidic chips to perform IF experiments. One chip was designed to screen the staining conditions and to take time-lapse images of protein expression in cells. The other was designed to perform high-throughput analysis of different cell lines. Both chips were made from PDMS with monolithically embedded pneumatic valves to control and reroute the liquid flow. These micro-valves were also critical components to isolate chambers, creating microenvironments without crosstalk.

We integrated all liquid handling steps of staining, including fixation, antibody incubation, and washing, onto a single chip, as shown in Fig. 1. The six fluid inlets (Fig. 1b, Inlet 1–6) on the left side of the chip were designed to deliver extra cellular matrix (*e.g.* fibronectin), cell suspension, culture medium, fixation solution, and other reagents. This chip had an interconnected fluidic channel network (blue channels in Fig. 1a, b), which could be formed as a long winding channel (Fig. 1c) or be divided and rearranged into 16 separated winding sections (Fig. 1d, e) by changing the configuration of the valves. The width of the fluidic channel is 300 μm , and the height is 25 μm . When the chip was configured as a 16-chamber format, each chamber had an individual inlet (*e.g.* Inlet 8 in Fig. 1b), and all chambers could also share a common inlet (Inlet 7 in Fig. 1b). Thus all chambers could be either operated fully independently from each other (Fig. 1d), or in parallel (Fig. 1e) when necessary, to reduce the tubing connections between reagents to the chip. With this chip, we tried different concentrations of primary and secondary antibodies, different incubation time spans, and different choices and concentrations of detergents during permeabilizing and washing steps, to optimize the labeling protocol on chip. Every batch of the 16 tests was carried out simultaneously on a single chip to identify the best conditions for observing specific localization of a given protein in a certain type of cell. To completely eliminate cross-contamination between conditions, we designed an extra washing channel through inlet 7 to flush off the previous solution before adding a new reagent.

To screen the proper concentration of primary antibody, we loaded and cultured NRK cells inside the channels and completely replaced the medium to PBS, and then fixed the cells. The cells were loaded through one of the inlets in the left side. With properly controlled cell density of the suspension, we have achieved uniform distribution of cells among all chambers, although this uniformity is not required for image-based analysis. After fixation, the cells were rinsed with PBS and then blocked. The chamber valves were then closed to form separated compartments and the cells were exposed to different concentrations of primary antibody through the top of inlet 8. After incubation, we reconfigured the control valves and rinsed the cells by washing buffer through the top of inlet 7. Finally, the cells were stained with secondary antibodies from the inlets on the left hand side, and rinsed with washing buffer again to complete the process.

We chose LAMP1, which had been proven as a proper immunological and biochemical marker of lysosome,³⁰ as our

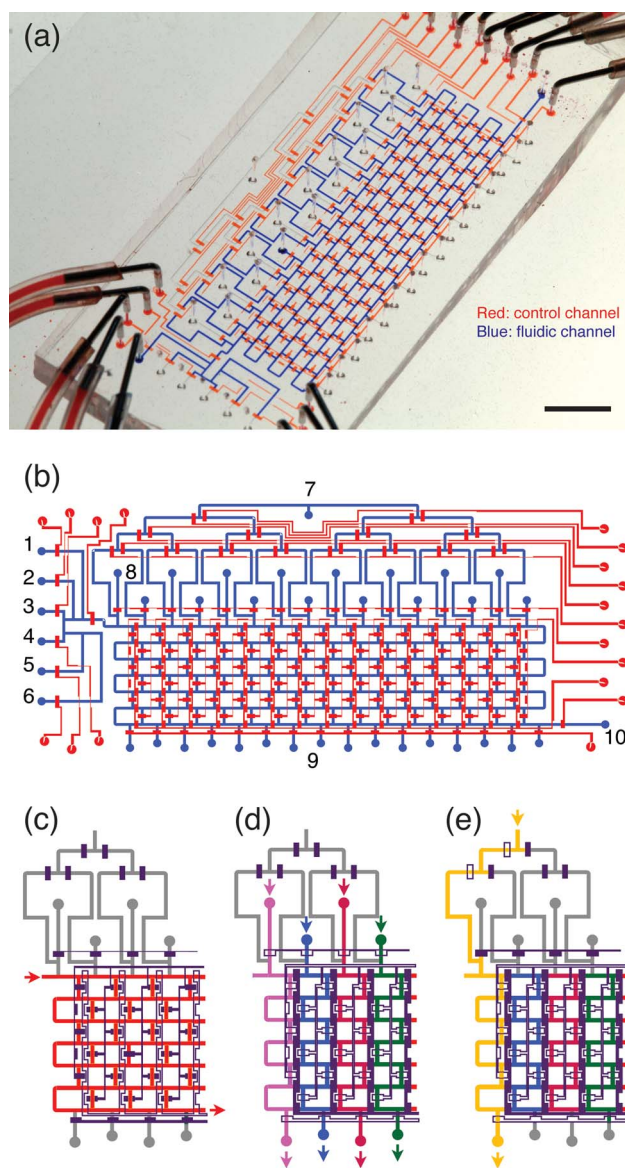


Fig. 1 A reconfigurable microfluidic chip for optimizing the experimental conditions of IF staining. (a) A microphotograph of a multilayer PDMS chip. The channels are filled with dyes to illustrate different layers in the chip. Scale bar is 5 mm. (b) The design layout of the chip. Inlets 1–8 are for sample and reagent introduction, inlet 9 and 10 are exit ports. (c) Chip configuration for cell loading. (d) Chip has been reconfigured to apply 16 different treatments in parallel. (e) Chip configuration for washing. Only a partial area of a chip is shown in (c)–(e). The valves are switched on (open channels in the figures) and off (filled channels in the figure) to perform fluidic rerouting.

target protein. The concentration is critical for staining. The concentrations of primary antibody of LAMP1 we tested were 2 $\mu\text{g mL}^{-1}$, 4 $\mu\text{g mL}^{-1}$, 10 $\mu\text{g mL}^{-1}$, or 20 $\mu\text{g mL}^{-1}$, and the corresponding concentrations of secondary antibody (FITC or TRITC conjugated IgG) were 1 $\mu\text{g mL}^{-1}$ or 2 $\mu\text{g mL}^{-1}$ respectively, and the incubation time was 30 or 60 min. We found that the optimal condition was 10 $\mu\text{g mL}^{-1}$ LAMP1 antibody with 2 $\mu\text{g mL}^{-1}$ secondary antibody, and that increasing incubation time from 30 to 60 min did not make any noticeable improvement.

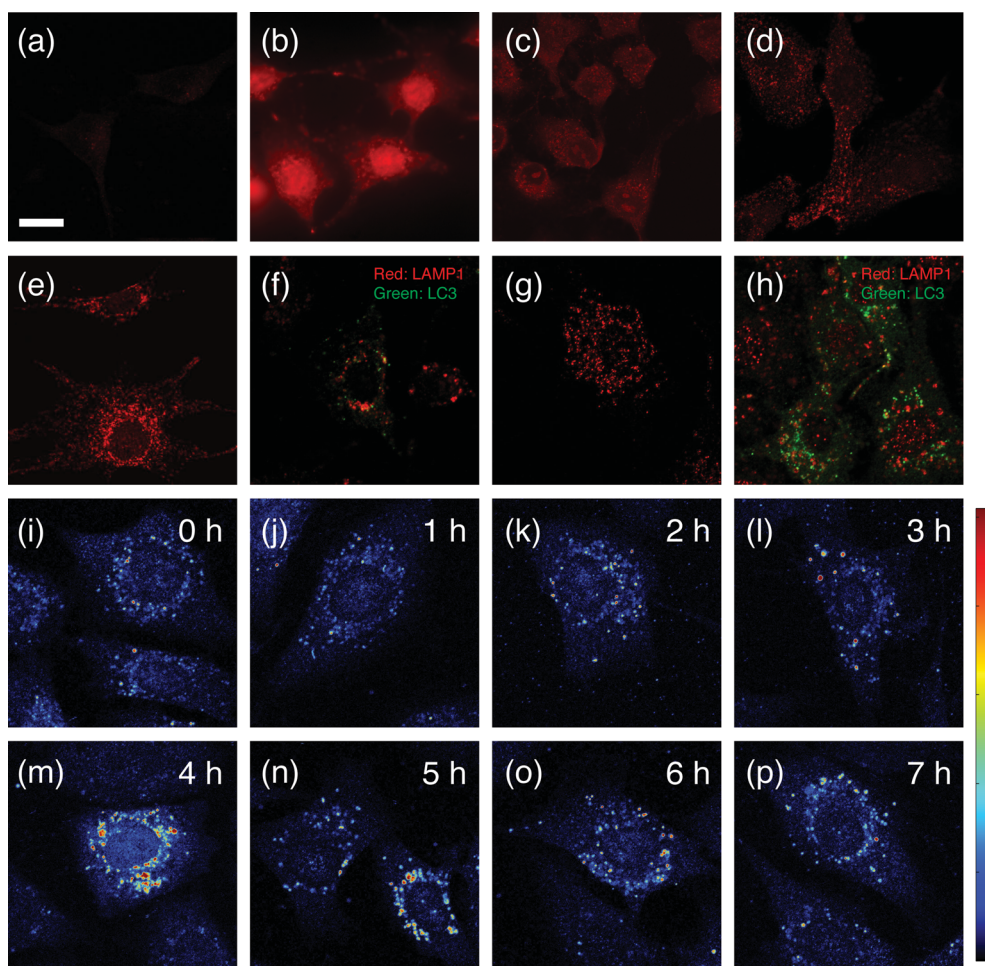


Fig. 2 Confocal images of IF staining under various experimental conditions. Unless specifically identified, the images were taken from the chip-based assay. (a) $4 \mu\text{g mL}^{-1}$ LAMP1 Ab; (b) $20 \mu\text{g mL}^{-1}$ LAMP1 Ab; (c) without detergent; (d) $10 \mu\text{g mL}^{-1}$ LAMP1 Ab with 1% Tween 20; (e) LAMP1 single staining; (f) LAMP1/LC3 double staining; (g) LAMP1 single staining on-slide; (h) LAMP1/LC3 double staining on-slide. (i)–(p) Time-lapse images of LC3 reveal the dynamic process of autophagosome formation during starvation. Scale bar: $5 \mu\text{m}$.

$4 \mu\text{g mL}^{-1}$ LAMP1 antibody gave faint fluorescence, which was too weak to analyze (Fig. 2a). A higher concentration gave a stronger signal but over-staining would blur the details (Fig. 2b). Even when we had used the optimum concentrations of primary and secondary antibodies we still observed some nonspecific background, mainly located in the cell's nuclear region (Fig. 2c). We then tested the function of saponin supplemented in the blocking solution and Tween 20 in the washing buffer, and adjusted the washing time accordingly. Tween 20 in the washing buffer led to the elimination of almost all nonspecific signals, and 3 min of washing time was sufficient to obtain a clear background (Fig. 2d). Since both solutions of primary and secondary antibodies contained saponin, further addition of saponin didn't help in suppressing the background noises.

Careful washing was necessary to reduce non-specific binding. Although washing time from seconds to minutes after secondary antibody incubation did not lead to a significant difference in background fluorescence intensity, prolonged washing was likely to flush the cells off the surface of the culture chambers. In addition, the flow velocity of the washing step was also important. Typically, we drove the fluid with compressed air at

$0.01\text{--}0.02 \text{ MPa}$ to ensure modest shear force so that the cells would not detach from the surface. The flow velocity was around $20 \mu\text{l min}^{-1}$ through the microchannels and the shear force was $\sim 100 \text{ dynes cm}^{-2}$ under this condition.

Correct choice of detergent and proper concentrations of antibodies were determined by a few well-designed combinatorial experiments on-chip. This approach not only significantly reduced the time and the reagents needed for condition screening, but also offered a robust way to generate high-throughput and parallel experimental conditions to reduce experimental errors.

Comparison between microfluidic staining and conventional methods

We carried out two sets of IF staining experiments in parallel, one was chip-based, while the other was on glass slides. Fig. 2e and 2f show the confocal images taken from chip-based experiments while the corresponding images from conventional methods are presented in Fig. 2g and 2h. Panels (e) and (g) are single staining images of LAMP1 while panels (f) and (h) are

double staining images of LAMP1 with LC3 using fibroblast cells. Through both staining methods, LAMP1 shows uniform dispersion in the cytoplasmic region.

Double staining is essential in the biological analysis to verify the co-localization of two proteins or sub-cellular organelles.³³ It is often used to localize one protein by employing another known protein as a location marker. LC3 is a highly specific marker for autophagosomal membranes.³⁴ The quantification of autolysosomes, measured by the double staining of LAMP1 and LC3, indicates the efficiency of the autophagosome–lysosome fusion.³⁵ Recently, autophagy has also been identified as a potential cause for LSDs.⁶ Both approaches provide high quality labeling for confocal imaging. However, the integrated microfluidic platform shows various advantages over conventional methods, thanks to its simple liquid handling procedure, low consumption of samples and reagents, and automatic performance of parallel analysis, which is more precise and more reproducible than similar assays performed by hand.

Determination of autophagic activity of mammalian cells with YFP-LC3

One major advantage of microfluidic chips is the precise control of the device. We employed the same chip to study dynamical processes in cells by sequentially terminating the parallel experiments one chamber after another at a fixed time interval, followed by IF staining and confocal imaging. We applied the chip-based IF method to study autophagic dynamics in cells. Autophagy was up-regulated in response to nutrient starvation to maintain the cell homeostasis.³⁶ An alternative measurement of LC3 was easily carried out by IF staining of its fusion protein (GFP or its derivatives) at given time-points of serum-starvation.

We observed autophagosome dynamics in cells expressing YFP-LC3 by taking time-lapse images under a confocal microscope at 1 h interval throughout a 7 h period (Fig. 2, panels i to p). We found that the YFP-LC3 signal was very weak in the cytoplasm with only a few punctate dots in the first 3 h, then significantly increased and peaked at the 4th and 5th h, and later decreased to a lower level. Our results agreed with the data reported previously.³⁷

The fixation solution was delivered through inlet 7 at preset time points during the starvation. For every hour of starvation, we picked a chamber to fix. Each fixation step took 10 min and then the cells were rinsed and incubated in PBS until we added other reagents to continue the IF staining process for all chambers. This integrated microfluidic IF staining system was automatically controlled by a Labview program, showing its great potentials to save labor and to shorten the time interval, while providing more detailed data.

Performance of multiple IF staining on-chip automatically

We designed another chip (Fig. 3a) to automatically perform complete IF staining of multiple cell samples. Reagents were delivered from the left side and each one was assigned to a particular inlet. The introduction of each reagent was programmed, ensuring the identical treatment (culture, staining, and imaging) of all cells for quantitative comparison. Cells were loaded from the top inlets and each sample was delivered into

two winding chambers, one for staining and the other for serving as the negative control without adding the primary antibody.

Fig. 3b demonstrates a few key steps for liquid manipulation during the experiment: cell loading (I), fixation and washing (II), primary antibody incubation (III), and secondary antibody incubation and washing (IV). The open/close status of the valves A and B could switch the configuration of the liquid routes of the chip. Through this reconfigurable design and the automation of liquid handling, we obtained highly parallel results and multiple replicates from a single run. Each run took about 10 h in total, including 8 h for cell seeding and culture, and 2 h for IF staining.

High-throughput analysis of lysosomal storage disorder cell lines

We applied this high-throughput chip to study LSDs cell lines. On the left side of the chip, we placed 7 inlets to deliver surface treatment reagents, culture medium, fixation solution, blocking solution, primary and secondary antibodies, and wash buffer, respectively.

LSDs will cause substrate accumulation inside the lysosomes, eventually leading to cell dysfunction, which in turn may cause defects in many other important cellular processes such as signaling pathways, lipid metabolism, intracellular calcium homeostasis, as well as trafficking.³⁷ Although most LSDs are still very hard to control by medication and therefore fatal, recently certain LSDs can be treated by a few promising therapeutic methods.³⁸ However, to be effective, these treatments must be applied before the symptoms reach the irreversible stage.^{39–41} Apparently, presymptomatic diagnosis of LSDs is essential. Since LSDs are caused by the deficiency of either a particular lysosomal protein or some nonlysosomal proteins involved in lysosomal biogenesis, diagnosis and analysis of LSDs highly depend on protein detection inside the cells. The diagnosis is further complicated by the mutation of the genes of proteins in the lumen or membrane of lysosomes,⁶ which can alter the morphology of lysosomes and cause LSDs. Current strategies are mainly immunoassay of blood spots⁴² and tandem mass spectrometry^{43–45} which detect the quantity of LAMP1. However, these approaches are time and labor consuming and come with high cost of reagents.

Recently a digital microfluidic platform has been introduced into LSDs screening using multiplex enzyme assay.^{46–48} These digital microfluidic approaches are extremely valuable for identifying the quantity of specific proteins in the samples. Chip-based methods offered automatic liquid handling through an inexpensive method, generating comparable results to the bench-top equipment. However, digital microfluidic assays cannot represent the changes of sizes and the distribution patterns of lysosomes. Since these changes are common features of many LSDs cell lines, we believe they can be used as markers for LSDs diagnosis. Having evaluated the capability of the microfluidic chips to perform IF staining, we applied our microfluidic chips to a cell-based high-throughput analysis of LSDs. We stained 16 different cell samples (15 cell lines from human patients with different LSDs and 1 wild type fibroblast cell line as the control) on-chip automatically. The whole process of staining took 2 h and used 0.3 μ L solution of each antibody per cell line. Besides the quantification of LAMP1, the morphology and distribution of lysosomes in the cell marked by LAMP1 immunostaining were also useful to distinguish LSD cells from normal cells.

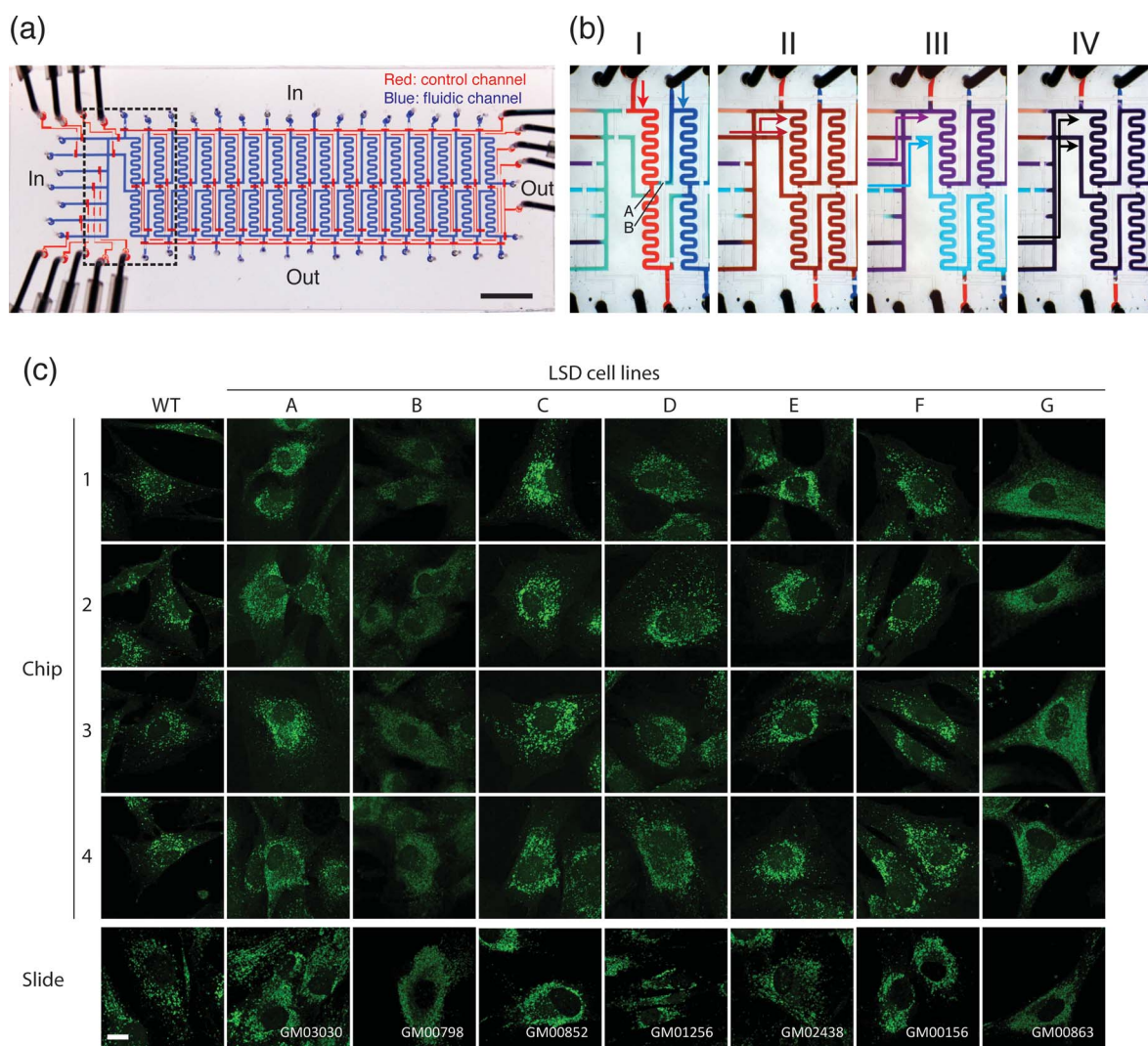


Fig. 3 A high-throughput IF chip for analyzing LSDs in parallel. (a) A 32-section chip could handle 16 different groups of cell samples in a single experimental run. Each experimental group had a control running in parallel. The scale bar is 5 mm. (b) Liquid flow in different steps could be reconfigured by integrated valves. I: cell loading; II: fixation and washing; III: primary antibody incubation; IV: secondary antibody incubation and washing. Valve A was used to separate the experimental groups and their control groups; valve B was used to isolate different samples. (c) Confocal images of LAMP1 immunofluorescence for different cell lines. We picked 4 representative images from each cell line that had been stained on-chip, and compared them with the result from conventional methods on glass slides. Wild type fibroblast cell lines was also shown in the first row as a control. Scale bar: 5 μm.

Fig. 3c compares 7 representative fluorescence images of different types of LSD cells, with the wild type fibroblast cell as the control, using both the microfluidic staining (upper 4 rows) and the conventional method (lower row). Among these cell lines samples, WT was the wild type cell; sample A was from a patient of X-linked ichthyosis; samples B and C were classified as disorders of lipid metabolism, namely Gaucher disease type III and Wolman disease, respectively; and the last four cell lines were from patients suffering from disorders of carbohydrate metabolism: mucopolysaccharidosis type I (MPS I), Hurler syndrome, neuraminidase deficiency with betagalactosidase deficiency, and MPS type IIIB.

We quantitatively analyzed the LAMP1 fluorescence spots by home-developed Matlab scripts. Almost all cells from the same cell line were identical with our chip-based IF method. For each

cell line, we randomly picked 4 isolated cells to analyze. The patterns (such as morphology and spot sizes, etc) of the cellular distribution of lysosome in LSD cells were very different from the wild type cells in terms of the number, size, spatial distribution, as well as the intensity of fluorescent spots.

Wild type cells usually show even distribution of small dots in the cytoplasm. One common feature of the LSDs cell lines is the increased number of the LAMP1 fluorescence spots, as shown in Fig. 4a. However, the spot counts can barely differentiate the different disease cell lines. Besides, it is difficult to obtain exact counts of the fluorescence spots using fully automatic image processing without manually separating some connected or overlapped spots. In some cell lines, the distribution patterns of the spots are very unique, giving us another dimension to differentiate certain diseases from the

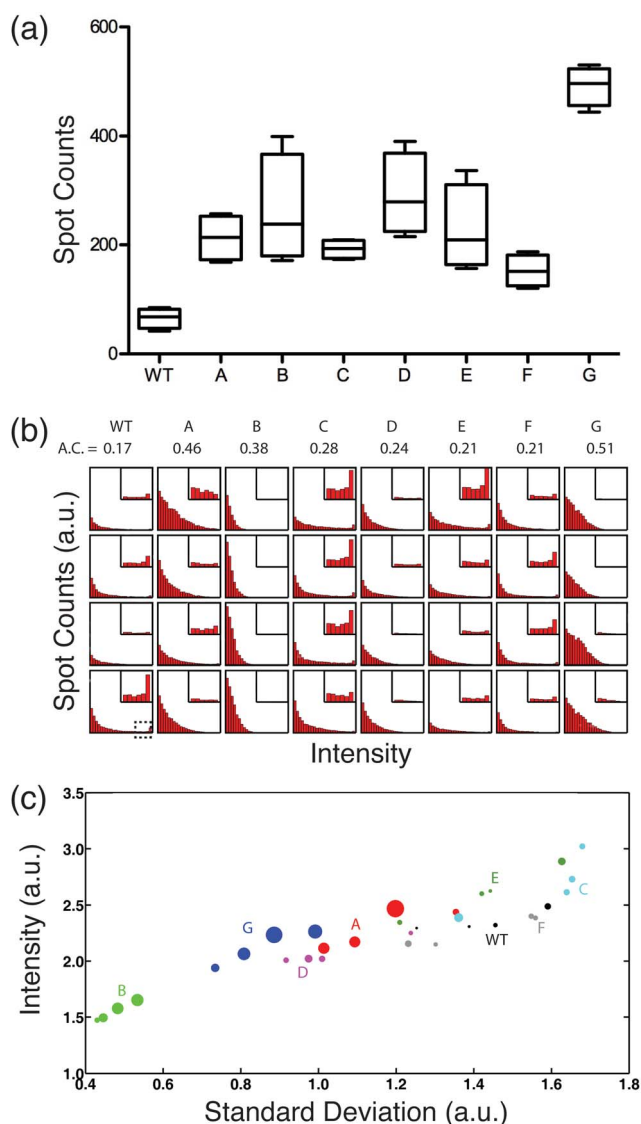


Fig. 4 Quantitative analysis of the fluorescent images of LAMP1 immunostaining for each cell line, including wild type (WT) and 7 different LSDs cell lines (A–G). (a) The single-cell fluorescent spot counts for each cell line. (b) The fluorescent intensity histogram of each cell. The intensity is divided into 30 levels, 25 fluorescent signal bars out of a total 30 bars are shown. Insets: distribution of the 6 brightest bars. (c) Scatter plot of the average intensity of LAMP1 fluorescence and the standard deviation of the intensity in each cell. The coverage rate of lysosome spots is indicated by the dot size in Fig. 4c.

others. For example, in sample F, lysosome spots show anisotropic distribution along the long axis of the nucleus, while in sample E, 85% of the lysosome spots locate in the 35% part of the cell close to the nucleus. However, most cell lines do not have these special patterns. Another significant feature of the fluorescent spots is the size. For example, the size of the spot in sample A is significantly smaller than that of WT cells (~30% reduction in terms of average area of single spots). Agglomerate spots appear in both samples C and E, with size increases of 1.5 and 1.2 times, respectively, compared to the WT cells.

We find that a better criterion to separate these cell lines is the combination of the fluorescence intensity of the spot, the distribution of the spots, and the distribution of the fluorescence intensity. We present the intensity histogram of each cell in Fig. 4b. For each cell, we divided the intensity into 30 levels, shown as bars in the histogram. Each histogram has been normalized by the total area of the cell under analysis. The background (dark area) counts have been removed from the histogram, thus all the bars presented in the figure reflect the signal from fluorescent spots. The average coverage (A.C.) of the fluorescent spots, calculated from the integrated area of those bars in the histogram, is also listed in the figure. Clearly all samples have larger coverage than WT cells, and samples A, B, and G are the samples with the highest coverage. Among these samples, cell line B is more uniform but has weaker fluorescent spots. The insets in the figure show the counts of the brightest fluorescent spots. The major difference between samples A and G is that A usually has brighter fluorescent spots. From the histogram we also find that with similar coverage, cell line C has brighter spots while cell line D has less bright spots than WT cells. Cell lines E and F are quite similar to WT cells in general but they can be easily separated from WT due to the unique spatial distribution pattern described above.

Based on what we have learned above, we try to use LAMP1 IF intensity, the standard deviation of the IF intensity, and the coverage of lysosome spots as three parameters to cluster the images of cells. As shown in Fig. 4c, in samples A, B, and G, the standard deviation of the intensity is smaller than the WT cell, and the coverage rate of lysosome spots is larger, as indicated by the dot size in the figure. In sample C, the average LAMP1 intensity is generally larger than the WT cell. In sample D, the intensity varies in a smaller range, which makes the standard deviation of the intensity smaller than the WT cell. Typically, the cells in each cell line can be well clustered by the average intensity and the standard deviation. Samples E and F have similar intensity and standard deviation to the intensity of the WT cell, and can be further identified by the anisotropic distribution of the spots. These clustering methods clearly hold great potential for early diagnosis and analysis of LSDs. The integrated microfluidic IF system will further facilitate this application by simultaneously detecting multiple target proteins and enzymes with small amount of cell samples in a single experimental run. All the experiments of disease cell lines were biologically duplicated, and WT cells were tested many times. Results of the same cell lines from different runs were nearly identical.

Conclusions

We have developed a microfluidic device to perform multi-step IF experiments and applied this method to analyze the lysosomal storage disorders cell lines. This method is ideal for optimizing experimental conditions and observing dynamic processes in cells with a much lower consumption of samples and reagents than conventional methods. The chip-based approach is also capable of preserving the high-quality IF images of cellular organelles for diseases diagnosis and analysis, and to investigate dynamic colocalization of proteins within cells through automatic double and multiple staining.

Acknowledgements

This work was funded by the National Natural Science Foundation of China (20733001, 20890020, 90913011, 20905004), the Ministry of Science and Technology of China (2007CB714502, 2009AA04Z309, 2011CB809106), and the Ministry of Education of China.

References

- 1 S. Iwamoto, R. C. Burrows, D. E. Born, M. Piepkorn and M. Bothwell, *Biomol. Eng.*, 2000, **17**, 17–22.
- 2 B. T. Bennett, J. Bewersdorf and K. L. Knight, *Methods*, 2009, **48**, 63–71.
- 3 P. Yager, T. Edwards, E. Fu, K. Helton, K. Nelson, M. R. Tam and B. H. Weigl, *Nature*, 2006, **442**, 412–418.
- 4 E. Lundberg and M. Uhlen, *Proteomics*, 2010, **10**, 3984–3996.
- 5 G. Liao, Y. Yao, J. Liu, S. Cheung and A. Xie, *J. Neurochem*, 2007, **102**, 36–36.
- 6 L. Yu, C. K. McPhee, L. Zheng, G. A. Mardones, Y. Rong, J. Peng, N. Mi, Y. Zhao, Z. Liu, F. Wan, D. W. Hailey, V. Oorschot, J. Klumperman, E. H. Baehrecke and M. J. Lenardo, *Nature*, 2010, **465**, 942–946.
- 7 E. F. Neufeld, *Annu. Rev. Biochem.*, 1991, **60**, 257–280.
- 8 A. H. Futerman and G. van Meer, *Nat. Rev. Mol. Cell Biol.*, 2004, **5**, 554–565.
- 9 T. Wennekes, R. J. van den Berg, R. G. Boot, G. A. van der Marel, H. S. Overkleeft and J. M. Aerts, *Angew. Chem., Int. Ed.*, 2009, **48**, 8848–8869.
- 10 P. Poncelet and P. Carayon, *J. Immunol. Methods*, 1985, **85**, 65–74.
- 11 G. M. Whitesides, J. C. McDonald and S. J. Metallo, *Anal. Chem.*, 2001, **73**, 5645–5650.
- 12 S. R. Quake and J. W. Hong, *Nat. Biotechnol.*, 2003, **21**, 1179–1183.
- 13 J. W. Hong, V. Studer, G. Hang, W. F. Anderson and S. R. Quake, *Nat. Biotechnol.*, 2004, **22**, 435–439.
- 14 S. R. Quake, M. A. Unger, H. P. Chou, T. Thorsen and A. Scherer, *Science*, 2000, **288**, 113–116.
- 15 S. R. Quake, T. Thorsen and S. J. Maerkl, *Science*, 2002, **298**, 580–584.
- 16 S. R. Quake, R. Gomez-Sjoberg, A. A. Leyrat, D. M. Pirone and C. S. Chen, *Anal. Chem.*, 2007, **79**, 8557–8563.
- 17 J. S. Glenn, S. Einav, D. Gerber, P. D. Bryson, E. H. Sklan, M. Elazar, S. J. Maerkl and S. R. Quake, *Nat. Biotechnol.*, 2008, **26**, 1019–1027.
- 18 N. Ye, J. Qin, W. Shi, X. Liu and B. Lin, *Lab Chip*, 2007, **7**, 1696–1704.
- 19 K. Hosokawa, M. Omata and M. Maeda, *Anal. Chem.*, 2007, **79**, 6000–6004.
- 20 K. Hosokawa, M. Omata, K. Sato and M. Maeda, *Lab Chip*, 2006, **6**, 236–241.
- 21 J. H. Qin, J. Kong, L. Jiang, X. O. Su, Y. G. Du and B. C. Lin, *Lab Chip*, 2009, **9**, 1541–1547.
- 22 E. P. Kartalov, J. F. Zhang, A. Scherer, S. R. Quake, C. R. Talyor and W. F. Anderson, *BioTechniques*, 2006, **40**, 85–90.
- 23 R. Wiedler, E. Fitzpatrick, S. McBride, J. Yavelow, S. Najmi and P. Zanzucchi, *Clin. Chem.*, 2006, **52**, 1080–1088.
- 24 J. T. McDevitt, S. E. Weigum, P. N. Floriano and N. Christodoulides, *Lab Chip*, 2007, **7**, 995–1003.
- 25 W. W. Liu, J. Goodhouse, N. L. Jeon and L. W. Enquist, *PLoS One*, 2008, **3**.
- 26 G. B. Lee, H. W. Wu, X. Z. Lin and S. M. Hwang, *Biomed. Microdevices*, 2009, **11**, 869–881.
- 27 J. S. Dordick, T. G. Fernandes, S. J. Kwon, M. Y. Lee, D. S. Clark and J. M. S. Cabral, *Anal. Chem.*, 2008, **80**, 6633–6639.
- 28 A. Levchenko, R. Cheong and C. J. Wang, *Mol. Cell. Proteomics*, 2009, **8**, 433–442.
- 29 E. L. Eskelinen, *Mol. Aspects Med.*, 2006, **27**, 495–502.
- 30 A. Ballabio, C. Settembre, A. Fraldi, L. Jahreiss, C. Spampanato, C. Venturi, D. Medina, R. de Pablo, C. Tacchetti and D. C. Rubinsztein, *Human Molecular Genetics*, 2008, **17**, 119–129.
- 31 E. Kominami, I. Tanida and T. Ueno, *Int. J. Biochem. Cell Biol.*, 2004, **36**, 2503–2518.
- 32 M. A. Unger, H. P. Chou, T. Thorsen, A. Scherer and S. R. Quake, *Science*, 2000, **288**, 113–116.
- 33 S. X. H. Lin and C. A. Collins, *J Cell Sci*, 1992, **101**, 125–137.
- 34 N. Mizushima, A. Yamamoto, M. Matsui, T. Yoshimori and Y. Ohsumi, *Mol. Biol. Cell*, 2004, **15**, 1101–1111.
- 35 N. Raben, L. Shea, V. Hill and P. Plotz, *Methods Enzymol.*, 2009, **453**, 417–449.
- 36 Z. Elazar, E. Fass, E. Shvets, I. Degani and K. Hirschberg, *J. Biol. Chem.*, 2006, **281**, 36303–36316.
- 37 V. Gieselmann and A. Ballabio, *Bba-Mol Cell Res*, 2009, **1793**, 684–696.
- 38 T. D. Butters, H. R. Mellor, K. Narita, R. A. Dwek and F. M. Platt, *Philos. Trans. R. Soc. London, Ser. B*, 2003, **358**, 927–945.
- 39 R. J. Desnick and E. H. Schuchman, *Nat. Rev. Genet.*, 2003, **4**, 157–157.
- 40 G. A. Grabowski and R. J. Hopkin, *Annu. Rev. Genomics Hum. Genet.*, 2003, **4**, 403–436.
- 41 R. J. Desnick, *J. Inherited Metab. Dis.*, 2004, **27**, 385–410.
- 42 M. S. Rashed, M. P. Bucknall, D. Little, A. Awad, M. Jacob, M. Alamoudi, M. Alwattar and P. T. Ozand, *Clinical Chemistry*, 1997, **43**, 1129–1141.
- 43 M. H. Gelb, F. Turecek, C. R. Scott and N. A. Chamoles, *J. Inherited Metab. Dis.*, 2006, **29**, 397–404.
- 44 D. S. Millington, N. Kodo, D. L. Norwood and C. R. Roe, *J. Inherited Metab. Dis.*, 1990, **13**, 321–324.
- 45 J. Herman, D. C. Kasper, V. R. De Jesus, T. P. Mechtler, T. F. Metz and B. Shushan, *Rapid Commun. Mass Spectrom.*, 2010, **24**, 986–994.
- 46 V. Pamula, R. Sista, Z. S. Hua, P. Thwar, A. Sudarsan, V. Srinivasan, A. Eckhardt and M. Pollack, *Lab Chip*, 2008, **8**, 2091–2104.
- 47 R. S. Sista, A. E. Eckhardt, T. Wang, C. Graham, J. L. Rouse, S. M. Norton, V. Srinivasan, M. G. Pollack, A. A. Tolun, D. Bali, D. S. Millington and V. K. Pamula, *Clin. Chem.*, 2011, **57**, 1444.
- 48 D. S. Millington, R. Sista, A. Eckhardt, J. Rouse, D. Bali, R. Goldberg, M. Cotten, R. Buckley and V. Pamula, *Semin. Perinatol.*, 2010, **34**, 163–169.